

# Various Three-Dimensional Structures Connected by Al–O/OH/Acetate–Al Bonds

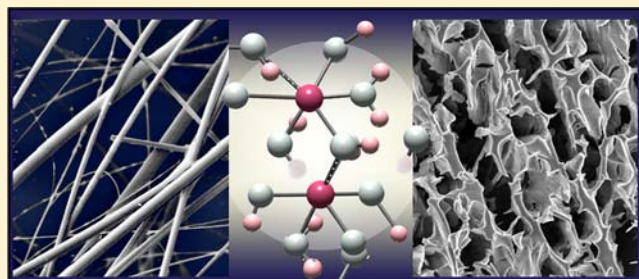
Katalin Sinkó,<sup>\*,†</sup> Shiro Kubuki,<sup>‡</sup> and Herwig Peterlik<sup>§</sup>

<sup>†</sup>Institute of Chemistry, L. Eötvös University, Budapest, H-1117, Hungary

<sup>‡</sup>Department of Chemistry, Graduate School of Science and Engineering, Tokyo Metropolitan University, Tokyo, 192-0397, Japan

<sup>§</sup>Faculty of Physics, University of Vienna, A-1090 Vienna, Austria

**ABSTRACT:** In the present work, significantly various structures connected by Al–O/OH/acetate–Al bonds were synthesized in a versatile sol–gel route. The various bond systems result in several three-dimensional (e.g., fibrous, highly porous, and compact) macrostructures. The shared acetate and OH ions provide the fibrous character; the shared OH ions and oxygen-bridges between octahedral Al(III) ions assist in the formation of a porous network; and the oxygen-bridges between differently (octa-, tetra-, and pentahedrally) coordinated Al(III) ions characterize the compact structures. The newly developed synthesis route is a fast and low-energy consumption sol–gel technique. This method applies only two starting materials and does not adopt any basic agent or catalyst. The synthesis is fast because it does not require any time-consuming peptization; a 3-D network forms directly from the initial solution. The low energy consumption arises from the low temperature of reactions (80 °C) and heat treatment (400–600 °C).



## INTRODUCTION

The present work represents the effectiveness of the liquid-phase syntheses to tailor the structure of the materials. The aluminum-containing materials are of particular interest for applications such as catalysts, membranes, adsorbents, ion exchangers, refractories, and implants owing to their thermal, chemical, and mechanical stability.<sup>1–5</sup> In the present work, various three-dimensional structures linked by Al–O/OH/acetate bonds were synthesized by a liquid-phase (sol–gel) technique. The usual sol–gel route means the hydrolysis of an Al-containing precursor and the condensation of the hydrolyzed Al compounds. The most frequently used Al precursors are aluminum isopropoxide and aluminum *sec*-butoxide.<sup>6–16</sup> The Yoldas process is the best known method for synthesizing aluminum oxide from aluminum alkoxides. The first step of the Yoldas method is the formation of boehmite sols by hydrolyzing aluminum-*sec*-butoxide in an excessively large amount of water, followed by a time-consuming process of peptization with HNO<sub>3</sub>.<sup>6,7</sup> The gelation of the sol can be achieved by the evaporation of the solvent. The drying and heat treatment of the gels produce aluminum oxide.<sup>6,7</sup> Alumina sols can also be prepared by increasing the pH value of inorganic aluminum salt solutions with the addition of a base.<sup>17–20</sup> There are only a few examples for applying Al nitrate as a single precursor in the sol–gel technique.<sup>21–24</sup> The typical synthesis pathway using Al nitrate is the precipitation of aluminum salt with ammonia, yielding aluminum oxide hydroxide powders.<sup>25</sup> The use of Al nitrate generally does not result in transparent 3-D networks.

## METHODS

**<sup>27</sup>Al Magic-Angle Spinning Nuclear Magnetic Resonance Spectroscopy.** <sup>27</sup>Al MAS NMR measurements were carried out at room temperature on a BRUKER AVANCE DRX-500 NMR spectrometer (11.70 T) at 130.3182 MHz. A 52 mm BB{1H}CP/MAS probehead was used with a 7 mm ZrO<sub>2</sub>/Kel-F rotor. After a 10 μs X pulse (approx. 90° flip angle), data were acquired during 125 ms, followed by a 1 s relaxation delay; 128 FID were accumulated. The typical spectral width was 65 360 Hz (501.05 ppm). Data processing parameters: line broadening, 30 Hz; real spectrum size, 16 K data points. <sup>27</sup>Al chemical shifts were recorded with respect to Al(H<sub>2</sub>O)<sub>6</sub><sup>3+</sup> as an external reference. For evaluation, the spectra composed from broad signals were generally decomposed to Lorentz curves by WINFIT software.

**Small-Angle X-ray Scattering.** SAXS experiments were conducted on a laboratory equipment operated with a 5.4 kW rotating anode X-ray generator (Nanostar from Bruker AXS, Karlsruhe), a pinhole camera with a variable sample-to-detector distance (25–108 cm), and a 2D position sensitive detector (Vantec 2000, Bruker AXS). The gels were wrapped in vacuum tight foil. The two-dimensional spectra were corrected for parasitic pinhole scattering, as well as for the foil scattering. A 1D MYTHEN detector was used as a WAXS detector. The WAXS data were collected over the 2θ range of 7–30° with a step size of 0.0212°. Identification of phases was achieved by comparing the diffraction patterns with the standard PDF cards.

**Scanning Electron Microscopy.** The SEM images were obtained on an FEI Quanta 3D FEG scanning electron microscope (SEM). The SEM images were prepared by the Everhart–Thornley secondary electron detector (ETD); its ultimate resolution is 1–2 nm. Since the conductance of the particles investigated is high enough to remove the

Received: August 27, 2013

Published: October 25, 2013

electric charge accumulated on the surface, the SEM images were performed in high vacuum without any coverage on the specimen surface. For the best SEM visibility, the particles were deposited on a HOPG (graphite) substrate surface.

**Attenuated Total Reflectance (ATR) Fourier Transform Infrared (FTIR).** FTIR measurements were monitored on a Bruker IFS 55 instrument with a diamond ATR head (PIKE Technologies). All infrared spectra were collected over the range of wavenumbers of 4000–550  $\text{cm}^{-1}$ .

## RESULTS

**Synthesis and Products.** The present sol–gel technique starts from only two chemical compounds, from an aluminum salt (aluminum nitrate) and a solvent (1-propanol), and it does not adopt any basic agent. Varying the time and the temperature of the reactions and the treatments was enough to tailor compact, macroporous, transparent glasslike, highly porous, and fibrous systems (Figure 1). Figure 2 represents the

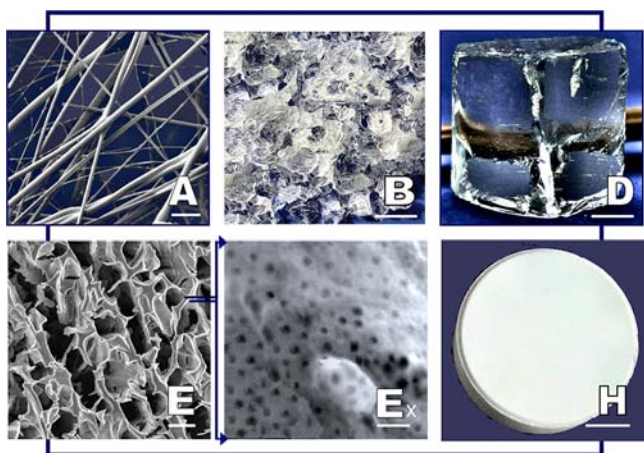


**Figure 1.** SEM images of the various macrostructures: (A) fibers; (B) macroporous; (D) transparent 3-D; (E) hierarchical porous; (H) compact systems. Magnification: the unit of “—” is 100 nm on (E<sub>x</sub>); 1  $\mu\text{m}$  on (A), 10  $\mu\text{m}$  on (E); 1 mm on (B); and 1 cm on (D) and (H).

outline of the syntheses, whereas Figure 3 characterizes the steps of the procedure and the chemical composition of the intermediate products. The essential difference between the 24 and 4 h treatments at 80 °C appears in the hydrolysis degree, 1.8 and 1.3, respectively. A transparent spinnable mixture (A) can only be obtained if the hydrolysis degree reaches the value of 1.8 (1.2 mol nitrate/Al) and the Al(III) concentration is 9.5 m/m% (Figures 2 and 3). This composition guarantees the spinnability. The system keeps its spinnability for several months. The fibers with diameters of 80–150 nm in Figure 1 can be produced by the electrospinning technique. The drawn fibers must be dried under close conditions in order to avoid their fracturing. The formation of a macroporous ( $\varnothing$ : 100  $\mu\text{m}$  to 1 mm) foam (B) from spinnable mixtures requires a 14 m/m% Al(III) concentration. Swelling of the macroporous foam in water results in an irreversible structural change, and a 3-D bond network forms (C). Although the swelling restores the composition of the spinnable mixture, the system still will not possess any spinnability. The volume of the water supplied to cause the swelling may be 10 times that of the macroporous foam at the most. Larger than the above amount of water destroys the 3-D network. The hydrogels (C) are good precursors to obtain monolith dried materials, transparent glass (D) by atmospheric drying, or highly porous systems (cryogel,

E) by freeze-drying (Figures 2 and 3). The cryogels can be characterized with a hierarchical pore structure and 45–80% porosity depending on the water content. The matrix is composed of interconnected cylindrical macropores with diameters of 1–2  $\mu\text{m}$  (Figure 1E). These pores are formed during the escape of ice crystals. The wall of macropores contains spherical pores with a diameter of 50–100 nm (Figure 1E<sub>x</sub>).

Considerable attention has been drawn to produce a compact  $\text{Al}_2\text{O}_3$  monolith by a low energy consuming method. The 24 h treatment of Al nitrate in *n*-propanol at 80 °C was too long for this aim due to the evolved high hydrolysis degree. The application of a 4 h treatment proved to be the most suitable for the procedure of a monolith with low porosity and high mechanical strength. The 4 h hydrolysis results in a viscous system (F), demonstrating a lower (1.3) hydrolysis degree (Figures 2 and 3). A porous, very hard product can be obtained

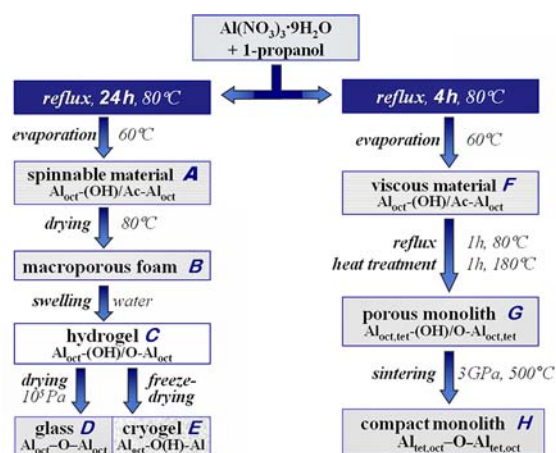


**Figure 2.** Outline of the syntheses:  $\text{Al}_{\text{oct}}$  octahedrally;  $\text{Al}_{\text{tet}}$  tetrahedrally coordinated Al(III).

by fast drying of the viscous system at 80 °C. Nevertheless, this hard product is destroyable by heating it to >300 °C owing to the gas release derived from the decomposition or combustion of N-containing compounds. The powders obtained from

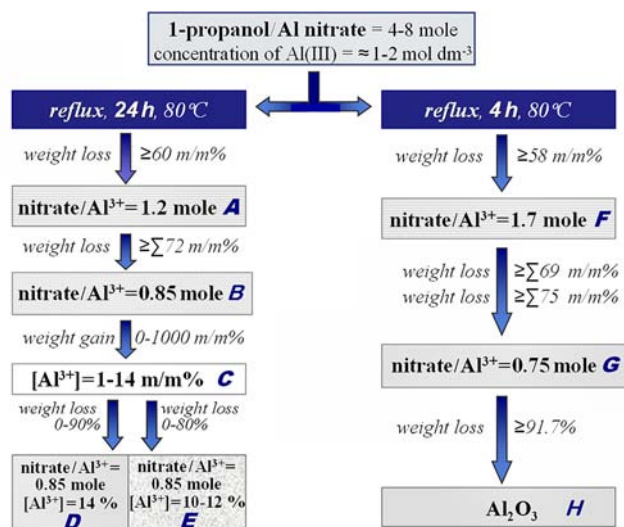


**Figure 3.** Chemical characterization of the syntheses.

cracking cannot be recompressed to a solid tablet. To avoid the cracking during the heat treatment, the gas evaporation must be carried out at the beginning of the drying, before the condensation reactions terminate. There are a lot of active groups on the surface treated only at low temperature; these groups are capable of reacting in further condensation reactions during the sintering. The major part of the nitrous gases escapes after a 1 h treatment in an open vessel at 80 °C, and the strongly bonded nitrogen compounds decompose when heated to 180 °C, producing a porous monolith (G). Sintering the monolith at 500 °C under pressure yields a compact Al<sub>2</sub>O<sub>3</sub> monolith (H) with high mechanical strength. Its Vickers hardness (VH) values are 180–200.

**Structure Investigations.** The bond systems demonstrate the variety of the synthesis products (Figure 4). In the

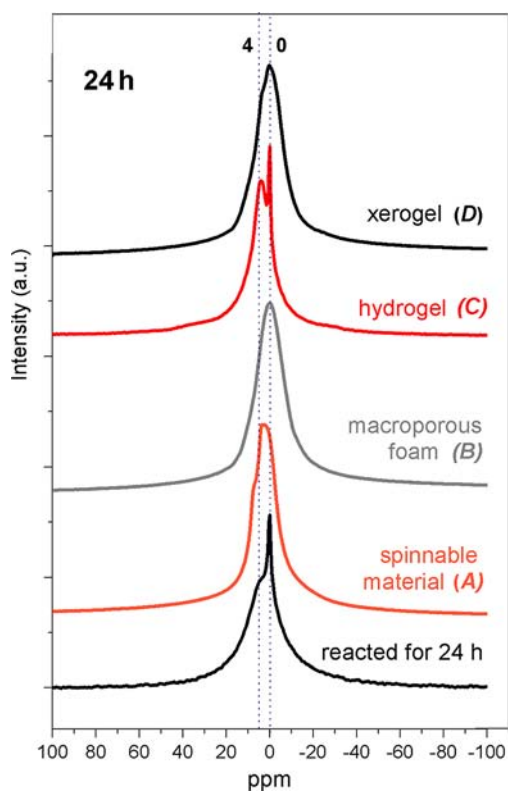


Figure 4. <sup>27</sup>Al MAS NMR spectra for systems of 24 h synthesis.

spinnable mixture (A), ~90% of the total Al ions are partially hydrolyzed octahedral Al(III) ions (0 ppm chemical shift in NMR spectrum<sup>27</sup>), and only 8–10% Al content is bonded in oligomers (3–4 ppm). Thus, only few and weak bonds (particularly through shared organic molecules and secondarily OH, H<sub>2</sub>O) can be identified in the mixture due to the large organic and small water content of the mixture. The broad NMR signal of the macroporous foam (B) indicates the conservation of the loose bond system of the viscous material; nevertheless, the hydrolysis process continues during the drying. In the hydrogels (C), 90% of the Al(III) ions are already octahedrally bonded in oligomers. The shared OH-/O- and acetate ions provide the connection in the Al-containing oligomers. The many OH-bridges formed by swelling modify the coordination sphere of Al ions irreversibly and terminate the spinnability. The NMR spectrum of dried hydrogels (glasslike xerogel, D, and cryogel, E) displays a more structured

signal than the dried spinnable material (B). The main part of aluminum (96–97%) is octahedrally bonded via OH-/O-bridges.

The structure of the system reacted for 4 h has been modified by drying it at 80 °C to boehmite-like ordering (Figure 5). The 5% octahedrally bonded Al ions can be

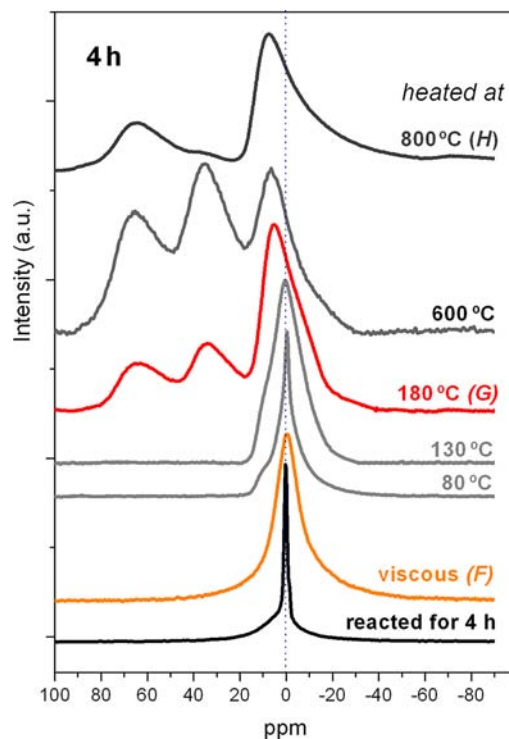


Figure 5. <sup>27</sup>Al MAS NMR spectra for systems of 4 h synthesis.

associated with the signal of amorphous or poorly crystalline boehmite at 9 ppm. A considerable change occurs in the atomic structure by heat treatment at 180 °C, justifying the importance of the 180 °C heating step. In the system obtained at 180 °C, there are octahedrally (5.2 ppm), pentahedrally (34 ppm), and tetrahedrally (63 ppm) bonded Al ions. This bond system essentially differs from the previous systems. Some aluminum oxide systems (e.g., pseudoboehmite) transform to 4-, 5-, and 6-coordinated Al-containing intermediates in the 200–600 °C range.<sup>26,28,29</sup> This atomic arrangement is preserved until the temperature of 600 °C; above 600 °C, it turns into various temporary Al<sub>2</sub>O<sub>3</sub> phases ( $\gamma$ -Al<sub>2</sub>O<sub>3</sub>,  $\eta$ -Al<sub>2</sub>O<sub>3</sub>,  $\gamma$ -Al<sub>2</sub>O<sub>3</sub>,  $\theta$ -Al<sub>2</sub>O<sub>3</sub>) and finally to  $\alpha$ -Al<sub>2</sub>O<sub>3</sub> (H).<sup>28</sup>

The XRD patterns also denote a sharp structural change around 180 °C and identify the presence of the boehmite phase and a small amount of Al hydroxide (Figure 6) at lower temperatures ( $\leq 180$  °C). The peaks of low intensity at 15° are attributed to the slight amount of various Al(OH)<sub>3</sub> and Al<sub>2</sub>O<sub>3</sub> phases; they do not indicate a homogeneous phase in the systems heated at >180 °C.

Studying the nanostructures, the SAXS curves follow the changes in the compositions more closely than NMR spectroscopy, especially in the water content (Figure 7). The scattering data indicate similar order in the systems of higher water content (A, C), whereas the dried systems (B, D) do not show any ordering. The partially hydrolyzed primary particles form isolated, isometric spherical units with a diameter of ~2.0 nm by 24 h of treatment at 80 °C, which is supported by the

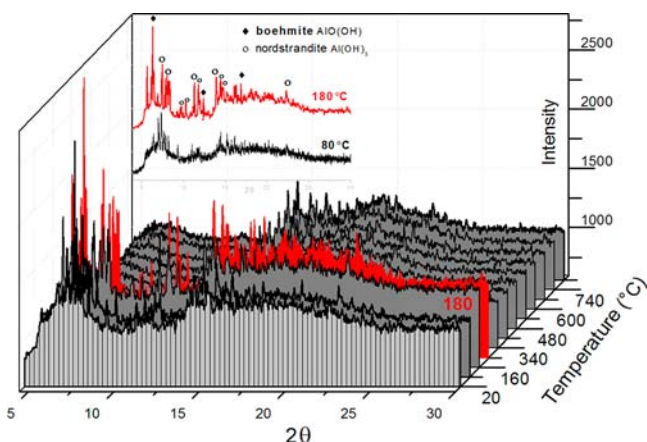


Figure 6. XRD pattern of system treated for 4 h vs temperature.

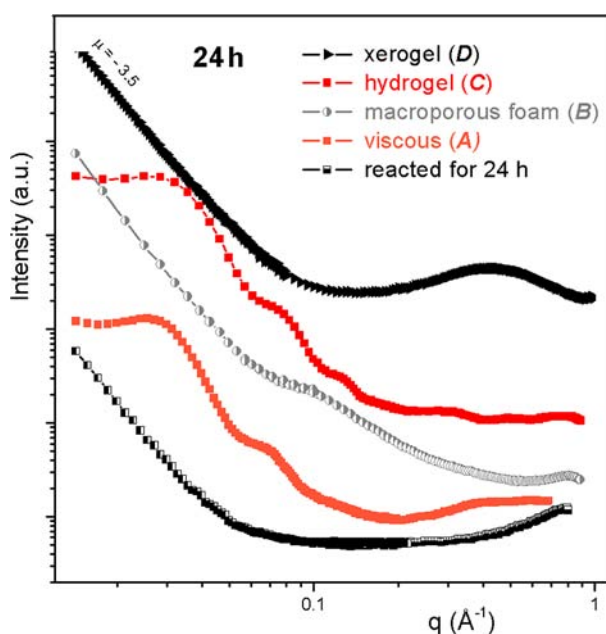


Figure 7. SAXS curves for systems of 24 h synthesis.

constant scattering intensity toward low  $q$ -values. The broad peaks lead to the conclusion that these units are linked to each other in a chainlike configuration at a typical distance of about 20 nm for the spinnable mixture (A) and at a little bit smaller distance of about 18 nm for the hydrogel, C. The swelling of the macroporous foam promotes the condensation processes and irreversibly transforms the structure built up from cylindrical units, resulting in a stronger 3-D network. Drying the hydrogel atmospherically yields a transparent glassy xerogel with a homogeneous aggregate structure. The systems derived from the 24 h treatment preserve the amorphous character up to 800 °C (XRD).

The SAXS data indicate some isolated primary units with the diameter of 2–3 nm in the samples reacted for 4 h, similar to the 24 h reacted system (Figure 8). The structural change at around 180 °C is also visible in the SAXS pattern. The SAXS data prove a more platelike structure, as concluded from the slope being close to 2 in the range between  $q = 0.02 \text{ \AA}^{-1}$  and  $q = 0.2 \text{ \AA}^{-1}$  for the samples heated  $\geq 180 \text{ °C}$ . The sharp peak at  $q = 0.78 \text{ \AA}^{-1}$  has been also identified by XRD as the first peak of the crystalline boehmite structure (Figure 8), viscous and 80

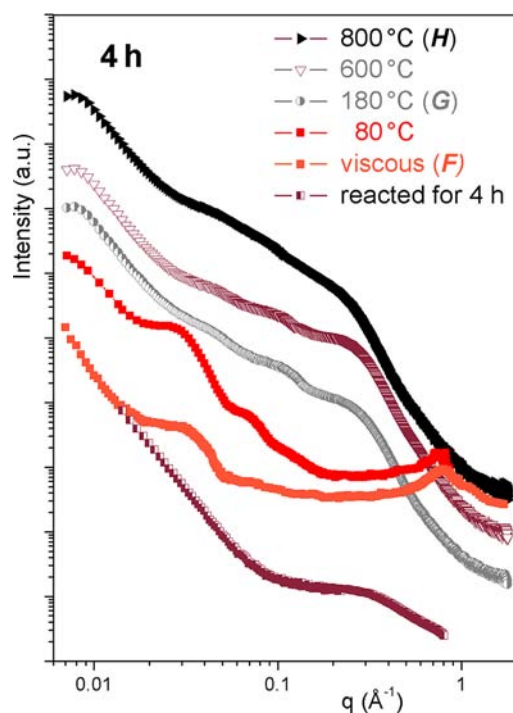


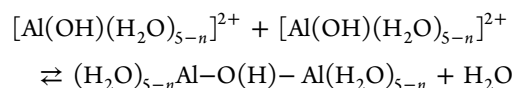
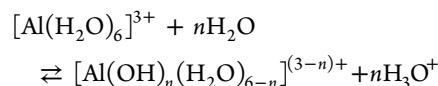
Figure 8. SAXS curves for systems of 4 h synthesis.

°C). At around 180 °C, the boehmite-like ordering transforms to intermediate Al oxide hydroxides detected by Al MAS NMR and XRD, as well. The intermediate Al oxide hydroxides possess slight ordering. The result of a fit curve can be interpreted as large plates with a Gaussian size distribution and a small additional structure factor to describe the weak tendency of the plates to agglomerate. The shift of the maximum on the SAXS curves represents the growth of the aggregate size in the function of the heat treatment, from 2 to 4 nm (300–400 °C) to 12–13 nm (600–800 °C).

## DISCUSSION

We developed a novel fast, low energy and cost consumption sol-gel technique for the preparation of various structures (fibrous, highly porous, and compact) connected by Al–O/OH/acetate–Al bonds. The novel method uses only two chemical compounds, an aluminum salt (aluminum nitrate) and a solvent (1-propanol), and it does not adopt any basic agent. The method is fast because it does not require any time-consuming peptization; a 3-D network forms directly from the initial solution. A washing step is not needed due to the lack of precipitations and the spontaneous decomposition of the nitrate content. The low energy consumption arises from the low reaction temperature (80 °C). The drying processes can be carried out at 80 °C and the heat treatment at 400–600 °C, respectively.

Two types of chemical reactions are performed during the gelation: hydrolysis and condensation, producing several oligomers.



The control of the hydrolysis degree of Al(III) ions proved to be the most efficient parameter in order to avoid the precipitation and to obtain a homogeneous gel system. The optimal hydrolysis degree of Al(III) ions for the synthesis is between 1.0 and 2.0. The  $>2$  hydrolysis degree generally leads to a precipitation, and the  $<1$  degree does not result in any 3-D network. Only a narrow range of the polarity and reaction temperature can be applied to achieve this transparent 3-D system using Al nitrate without any basic agent.

The optimal temperature for the condensation reactions is 75–80 °C. Above 80 °C, *n*-propanol boils; at lower temperatures, the reactions occur with an extremely low rate; and below 65 °C, the 3-D network does not form at all. The *n*-propanol provides the optimal polarity for the gelation. The treatment of Al nitrate in ethyl alcohol does not produce gels due to its too high polarity. Butyl alcohol is not able to dissolve Al nitrate.

The 1-propanol has several roles in the gelation processes. First; it dissolves the aluminum salt and, second, it reduces the polarity of the medium. In the less polar medium, the nitrate ions pick up H<sup>+</sup> ions yielded by the hydrolysis of Al<sup>3+</sup> and the nitric acid molecules decompose and escape as nitrous gases at 80 °C. (During the reflux at 75–80 °C, ~60% of the total nitrate content decomposes in *n*-propanol, 55% in ethanol, and 25% in methanol.) The removal of the nitric acid molecules increases the pH, which promotes the hydrolysis and condensation reactions. The hydrolysis degree (the OH/Al(III) ratio) increases by reduction of the nitrate content. The third role of *n*-propanol is a chemical reaction with nitric acid and/or its decomposition products producing acetate ions.<sup>27</sup> Figure 9 illustrates the nitrate- and Al-containing oligomer contents as a function of reaction time at 80 °C, proving the importance of the escape of nitrate ions.

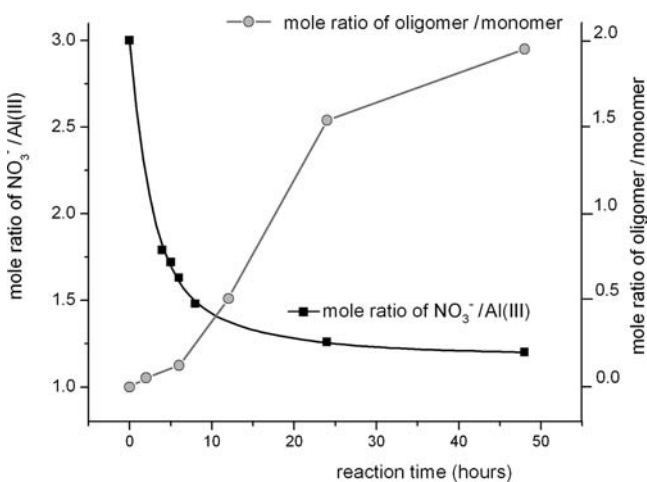


Figure 9. Nitrate and oligomer contents vs reaction time.

The nitric acid oxidizes 30% of the propanol content. The acetate coordination plays an important role in the formation of the 3-D network. Occupying the coordination sites, the acetate ions hinder the precipitation. The main part of Al atoms are involved in oligomers linked by OH, O, and/or acetate ions as bidentate ligands (Figures 10 and 11). AlO<sub>4</sub> units cannot be revealed by NMR or FTIR in the samples reacted for longer times. Both data indicate octahedrally bonded Al(III) ions rather than tetrahedrally ions. The absorption bands in the range of 3400–3200 cm<sup>-1</sup> verify the OH groups involved in H-

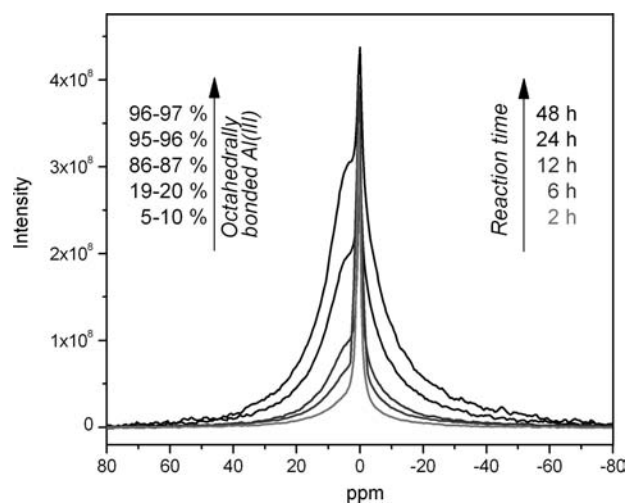


Figure 10. <sup>27</sup>Al MAS NMR spectra for systems prepared for various reaction times.

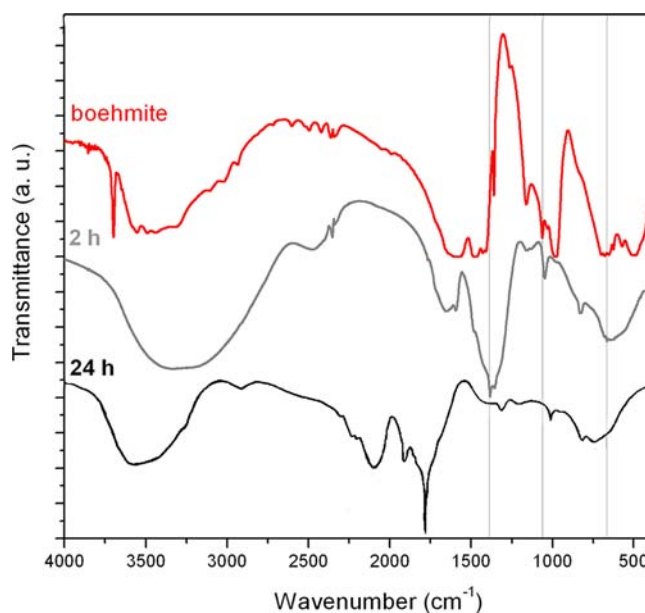


Figure 11. FTIR spectra for systems prepared for various reaction times.

bonds. The absorption peaks between 3450 and 3600 cm<sup>-1</sup> are derived from the free OH groups on the surface. The bands at 1417, 1472, and 1595 cm<sup>-1</sup> can be associated with acetate ions coordinated to Al(III) ions (Figure 11). The presence of the bidentate acetate ions has also been verified by the atmospheric pressure chemical ionization (APCI) MS technique. The peak at 1160 cm<sup>-1</sup> represents the Al–OH–Al bonds.<sup>28</sup>

Thus, the control of the hydrolysis degree has a decisive role in the variation of the material structures. A strongly limited chemical composition (1.8 hydrolysis degree; 9.5 m/m% Al(III) ions) is required for the excellent spinnability. Only 8–10% Al content is bonded in the aggregates of the spinnable system (A). The low water activity, large concentration, and the presence of the organic ligands favor the formation of cylindrical aggregates, which induce the good spinnability. Further treatment (drying and swelling) leads to an irreversible structural change due to the proceeding condensation reactions. The octahedrally bonded Al content (90%) in the hydrogels

proves the more condensation. Moreover, the bond system is also modified in the hydrogels (C); namely, OH/O-bridge connections are dominated rather than shared water molecules. The 3-D structure of the hydrogel provides as a starting material for various drying processes. In the dried products (glass and cryogels), 96–97% of Al(III) ions are octahedrally bonded by OH/O-bridges. The octahedral Al(III) ions can exist only on the surfaces of particles, whereas the tetrahedral coordination characterizes the Al ions in the inside. Thus, the presence of the octahedral Al ions considerably contributes to the porosity increase. The dried systems preserve their amorphous character up to 800 °C.

The lower hydrolysis degree (1.3) results in a boehmite-like ordering (Figure 11). This structure can be converted to various intermediate Al oxide hydroxide crystalline phases at higher temperature. Not only octahedral but also pentahedral as well as tetrahedral Al(III) ions can be identified in the monolith oxide systems. The bond systems (O-bridges) of the different coordinated Al(III) ions and the crystalline phases induce the high mechanical strength of the alumina material (H).

## CONCLUSIONS

In summary, a novel fast, low energy and cost consumption sol–gel technique has been evolved for preparation of various structures connected by Al–O/OH/acetate–Al bonds: nanofibrous, macroporous, hierarchical porous, and compact systems. The new method applies only two starting materials, aluminum nitrate and 1-propanol. It does not adopt any basic agent or catalyst. The low reaction and heat treatment temperatures (80 and 400–600 °C) provide the method with low energy requirements. This method is fast owing to the formation of 3-D networks directly from the initial solutions and the spontaneous decomposition of anions of Al salt.

The control of the hydrolysis degree of Al(III) ions is the most efficient parameter in order to avoid the precipitation and to obtain homogeneous systems. The bond system has an important role in the formation of various structures. Over the low water activity and the large Al concentration, the shared OH and acetate ions as bidentate ligands provide the outstanding spinnability. More than 95% of Al(III) ions are octahedrally bonded by OH/O-bridges in the highly porous materials, which can be utilized as an excellent insulation material or adsorbent. The bond systems of alumina monoliths with low porosity can be characterized by O-bridges between differently (tetra-, octa-, and pentahedrally) coordinated Al(III) ions. The alumina monoliths are eligible to be used as an implant or refractory material due to their high mechanical strength (180–200 HV) and heat resistance up to 1500 °C.

## AUTHOR INFORMATION

### Corresponding Author

\*E-mail: sinko@chem.elte.hu.

### Author Contributions

The manuscript was written through contributions of all authors. All authors have given approval to the final version of the manuscript.

### Notes

The authors declare no competing financial interest.

## ACKNOWLEDGMENTS

This study has been supported by EU FP-7 CHATT ACP1-GA-2011-285117 and OTKA NK 101704 funds.

## REFERENCES

- (1) Trimm, D. L.; Stanislaus, A. *Appl. Catal.* **1986**, *21*, 215–238.
- (2) Cejka, J. *Appl. Catal., A* **2003**, *254*, 327–338.
- (3) Richard, K. O. *Applied Industrial Catalysis*; Academic Press: New York, 1983; Vol. 3.
- (4) Maki, T.; Sakka, S. J. *Non-Cryst. Solids* **1988**, *100*, 303–308.
- (5) Gitzen, W. H. *Alumina as a Ceramic Material*; American Ceramic Society: Columbus, OH, 1970.
- (6) Yoldas, B. E. *J. Mater. Sci.* **1975**, *10*, 1856–1860.
- (7) Yoldas, B. E. *J. Am. Chem. Soc.* **1982**, *65*, 387–393.
- (8) Suh, D. J.; Park, T. J.; Kim, J. H.; Kim, K. L. *Chem. Mater.* **1997**, *9*, 1903–1905.
- (9) Pierre, A. C.; Elaloui, E.; Pajonk, G. M. *Langmuir* **1998**, *14*, 66–73.
- (10) Rolison, D. R.; Dunn, B. J. *Mater. Chem.* **2001**, *11*, 963–980.
- (11) Kureti, S.; Weisweiler, W. J. *Non-Cryst. Solids* **2002**, *303*, 253–261.
- (12) Carnes, C. L.; Kapoor, P. N.; Klabunde, K. J.; Bonevich, J. *Chem. Mater.* **2003**, *13*, 2922–2929.
- (13) Liu, S.; Fookan, U.; Burba, C. M.; Eastman, M. A.; Wehmschulte, R. J. *Chem. Mater.* **2003**, *15*, 2803–2808.
- (14) Wilcox, L.; Burnside, G.; Kiranga, B.; Shekhawat, R.; Mazumder, M. K.; Hawk, R. M.; Lindquist, D. A.; Burton, S. D. *Chem. Mater.* **2003**, *15*, 51–56.
- (15) Kim, Y.; Kim, C.; Kim, P.; Yi, J. J. *Non-Cryst. Solids* **2005**, *351*, 550–556.
- (16) May, M.; Navarrete, J.; Asomoza, M.; Gomez, R. J. *Porous Mater.* **2007**, *14*, 159–164.
- (17) Wood, T. E.; Siedle, A. R.; Hill, J. R.; Skarjune, R. P.; Goodbrake, C. *Mater. Res. Soc. Symp. Proc.* **1990**, *180*, 97–116.
- (18) Fu, G.; Nazar, L. F.; Bain, A. D. *Chem. Mater.* **1991**, *3*, 602–610.
- (19) Kurokawa, Y.; Suga, T.; Nakata, S.; Ikoma, T.; Tero-Kubota, S. J. *Mater. Sci. Lett.* **1998**, *17*, 275–278.
- (20) Zhang, Z.; Hicks, R. W.; Pauly, T. R.; Pinnavaia, T. J. *J. Am. Chem. Soc.* **2002**, *124*, 1592–1593.
- (21) Macêdo, M. I. F.; Osawa, C. C.; Bertran, C. A. *J. Sol-Gel Sci. Technol.* **2004**, *30*, 135–140.
- (22) Baumann, T. F.; Gash, A. E.; Chinn, S. C.; Sawvel, A. M.; Maxwell, R. S.; Satcher, J. H. *Chem. Mater.* **2005**, *17*, 395–401.
- (23) Pillai, K. T.; Kamat, R. V.; Mukerjee, S. K.; Vaidya, V. N. *BARC Newsl.* **2009**, *309*, 359–366.
- (24) Jiansirisomboon, S.; MacKenzie, K. J. D. *Mater. Res. Bull.* **2006**, *41*, 791–803.
- (25) Li, J. G.; Sun, X. *Acta Mater.* **2000**, *48*, 3103–3112.
- (26) Bradley, S. M.; Hanna, J. V. *J. Am. Chem. Soc.* **1994**, *116*, 7771–7783.
- (27) Mezei, R.; Karancsi, T.; Rohonczy, J.; Sinkó, K. J. *Mater. Chem.* **1998**, *8*, 2095–2101.
- (28) Ingram-Jones, V. J.; Slade, R. C. T.; Davies, T. W.; Southern, J. C.; Salvador, S. J. *Mater. Chem.* **1996**, *6*, 73–78.
- (29) Fitzgerald, J. J.; Piedra, G.; Dec, S. F.; Seger, M.; Maciel, G. E. J. *Am. Chem. Soc.* **1997**, *119*, 7832–7842.